Solar-Powered Critical Cooling:
A Theoretical Feasibility Study for Human Thermal Regulation

By

Jeff Hall
B.S. Mechanical Engineering, Michigan State University, 2017

Submitted to the Department of Mechanical Engineering
in partial fulfillment of the requirements for the degree of

MASTER OF SCIENCE IN MECHANICAL ENGINEERING
at the
MASSACHUSETTS INSTITUTE OF TECHNOLOGY

May 2025

Authored by: Jeff Hall
Department of Mechanical Engineering
May 6, 2025

Certified by: Christoph Reinhart
Department of Architecture
Terri and Alan Spoon Professor of Architecture and Climate
Thesis supervisor

Accepted by: Prof Nicolas Hadjiconstantinou
Chairman, Department Committee on Graduate Theses

Solar-Powered Critical Cooling:
A Theoretical Feasibility Study for Human Thermal Regulation

by
Jeff Hall

Submitted to the Department of Mechanical Engineering
in partial fulfillment of the requirements for the degree of
Master of Science in Mechanical Engineering

ABSTRACT

Over the last 50 years, the leading global environmental hazard has not been hurricanes, lightning, tornadoes, floods, or earthquakes, but extreme heat events. With climate models projecting an increase in the frequency, intensity, and duration of heatwaves in the coming decades this threat to life is expected to only increase. Air conditioning has been demonstrated to reduce mortality during heatwaves yet uses an order of magnitude more energy than necessary to keep a human cool. Using principles of similitude to extrapolate the capability of existing vapor compression equipment, an objective function to maintain energy balance in a human exposed to extreme heat is developed across a design space. The function shows that in a standard forced convection air conditioning system, there no opportunity to provide emergency cooling of a human due to the slow mass flow rate needed to cool air in a single stream. As such, status-quo attempts to cool humans with general-purpose air conditioning will always be an inefficient use of energy. By focusing on keeping people cool, not spaces, we propose three paths forward for critical human cooling that appropriately match the energy needs of humans: radiative cooling, liquid cooling devices, and low-mass flow air conditioning.

Thesis supervisor: Christoph Reinhart
Title: Terri and Alan Spoon Professor of Architecture and Climate

Table of Contents

LIST OF FIGURES **4**

LIST OF TABLES **5**

CHAPTER 1 - INTRODUCTION **6**

CHAPTER 2 - EVALUATION OF VAPOR-COMPRESSION CONVECTIVE COOLING **7**

Part 1: Defining System Requirements for Critical Cooling 7
Part 2: Equation development for convectively cooling a human using conditioned air 11
Determination of h in terms of physical parameters: 11
Part 3: Equation development for creating a low temperature airstream using a vapor compression cycle 14
Determination of mass flow rate and pressure ratio 16
Part 4: Relating T_{evap} and $T_{airstream}$ 18
Part 5: Examining air recirculation 22
Part 6: Mass flow rate minimization 24

CHAPTER 3 - DISCUSSION OF ALTERNATIVES **27**

Ice or Phase-Change Vest (Solid-State Cooling): 27
Circulating Liquid Vest or Chair: 28
Evaporation: 29
Radiation: 30
View factor between human and cooling device: 34
View factor between human and room: 34
View factor between cooling device and room: 34

CHAPTER 4 – DISCUSSION **37**

CHAPTER 5 - CONCLUSION **40**

BIBLIOGRAPHY **42**

List of Figures

Figure 2-1: Human cooling strategy using status-quo technology. A vapor compression cycle cools air to be blown at a hot subject 7
Figure 2-2: Thermodynamic system under review. Notice the single inlet, single outlet, constant ambient air temperature assumption inherent in the design. 11
Figure 2-3: Empirical Correlation of Airspeed and Convective Heat Transfer Coefficient for the Human Chest Oliveira et al. 2014 12
Figure 2-4: Computed air velocity as a function of airstream temperature and airstream area for convectively removing 72W. The upper bound of area is 1.8m2, the skin surface area of an average human. 12
Figure 2-5: Power law fit of a known fan dataset to the related non-dimensional parameters... 13
Figure 2-6: Computed fan power as a function of airstream temperature and airstream area for convectively removing 72W 14
Figure 2-7: Power draw of a hypothetical vapor compression cycle across reasonable mass flow and pressure ratio ranges 16
Figure 2-8: Power draw of a vapor compression cycle across evaporator temperatures after mass flow rate is solved 18
Figure 2-9: Minimum airspeed and temperature needed to convectively cool a human using a fan diameter approximately double the width of a human torso 19
Figure 2-10: Required heat transfer into air at the mass flow rates needed to convectively cool a human 20
Figure 2-11: Required heat transfer into air at the mass flow rates needed to convectively cool a human over a maximized surface area 20
Figure 2-12: Screenshot from Bardhan et al. 2024 showing home construction 22
Figure 2-13: Sample Window Air-Conditioners 23
Figure 2-14: Model for low mass flow rate design 25
Figure 3-1: Screenshot from Epstein, Shapiro, and Brill 1986 showing their calculation of cooling power of an ice vest. 27
Figure 3-2: Various cooling vests for sale on uline.com 28
Figure 3-3: Commercially available Personal Cooling Systems 28
Figure 3-4: Effective cooling rate calculated by Jette et al. 2004 for a commercially available cooling vest 29
Figure 3-5: Fan power to evaporatively remove 72W from different wetted areas of skin. Plot is showing 30 ℃ air with 25% RH. 30
Figure 3-6: Sensitivity analysis of the excess energy generated by the human showing high sensitivity to the variables in the radiation calculation 31
Figure 3-7: Net radiative heat transfer between a black body in a large black enclosure 32
Figure 3-8: Schematic of radiative cooling cylinder 33
Figure 3-9: Top-down view of cooling device with reflectors to increase view factor 34
Figure 3-10: Candidate chiller from RigidHVAC.com 36
Figure 3-11: Hypothetical implementation of radiative cooling device (generated with ChatGPT). Reflectors would need to be significantly larger than shown to achieve a view factor of 0.72... 36

List of Tables

Table 2-1: Material Properties and Measured Temperatures for Traditional African Settlement . 8
Table 2-2: Calculated Mean Radiant Temperature for Traditional African Settlement 8
Table 2-3: Meteorological Data for Kisumu, Kenya 8
Table 2-4: Physiological Parameters 9
Table 2-5: Calculated Heat Transfer From Human Body Inside Traditional African Settlement .. 9
Table 2-6: Photovoltaic Data 10
Table 2-7: Notation for Non-Dimensional Rotary Compressor Relationships 17
Table 2-8: Scaled Mass Flow Rate 17
Table 2-9: Air Density Change from 0℃ to 30℃ 19
Table 2-10: ClimateStudio Simulation Parameters 22
Table 2-11: Validation of ClimateStudio Model 22
Table 2-12: ClimateStudio Peak Day Simulation Results 23
Table 2-13: ClimateStudio Peak Power Draw Simulation Results 23
Table 2-14: Fan Power Requirements for Convective Cooling 24
Table 3-1: Parameters for three-body radiative exchange 35
Table 5-1: Comparison of Discussed Methods for Cooling a Human 41

Chapter 1 - Introduction

Over the last 50 years, the leading global environmental hazard has not been hurricanes, lightning, tornadoes, floods, or earthquakes, but extreme heat events (Coates et al. 2014). With climate models projecting an increase in the frequency, intensity, and duration of heatwaves in the coming decades (Perkins-Kirkpatrick and Lewis 2020) this threat to life is expected to only increase. In fact, the Harvard Law Human Rights Entrepreneurs Clinic has begun to establish cooling as a human right "derived from existing rights, such as the right to life, health, housing, and a clean and healthy environment…". While humans have sophisticated thermoregulatory mechanisms to maintain body temperature through these heat events, environmental or physiological conditions can compromise the available pathways for heat transfer and core temperature can rise to dangerous levels (Székely, Carletto, and Garami 2015).

Among the populations most at risk are the elderly, whose thermoregulatory responses are diminished with age (McKenna et al. 2023). In addition, studies have shown that conventional cooling methods, such as electric fans, are detrimental during extreme heat events (Morris et al. 2021). Air conditioning, in contrast, has been consistently associated with a reduced risk of heat related mortality across all ages (Semenza et al. 1996).

Despite this life-saving potential, air conditioning remains a product traditionally marketed and sold as a comfort-oriented, luxury good engineered to cool entire rooms and houses. In fact there is a direct correlation between per capita income of a nation and the number of installed air conditioning systems (IEA 2018). As a result, these systems are typically sized to cool a large volume of air, rather than an individual, and the resulting energy demands are accordingly an order of magnitude higher than required to maintain body temperature during heat stress. For example, a human at rest generates 100 watts of heat, yet the smallest widely available AC unit in the U.S. moves over 1400 watts of heat.

In the context of a warming world, air conditioning is undergoing a fundamental shift from a convenience to a necessity, more like a refrigerator than a dishwasher, an appliance with the power to save lives. Yet for many, particularly low-income individuals, the high upfront and operational costs of conventional AC systems remain prohibitive (Gowen et al. 2023). Compounding this issue, extreme heat events increasingly strain the electricity grid, leading to blackouts that render these life-saving systems useless precisely when they are most needed, substantially increasing the mortality rate from a heat wave alone (Stone et al. 2023). This lack of grid resilience exposes a dangerous dependency on centralized, high-power infrastructure for personal thermal safety.

To ensure affordable and reliable access to cooling we must re-evaluate the status-quo. This paper evaluates whether vapor-compression system designs, the dominant global air conditioning technology, can be redesigned to align with the physiological energy needs of humans and thus be compatible with resilient, off-grid power sources with a path towards equitable access.

Chapter 2 - Evaluation of Vapor-Compression Convective Cooling

Cooling a human during extreme heat, or what we will call “critical cooling” as a departure from comfort cooling, requires energy in some form to remove heat to compensate for a failure of our thermoregulatory mechanism. While there are many strategies to cool a human down, it is natural to start with an evaluation of the status-quo technology: an air conditioning system in which a fan both pulls air through a chilled heat exchanger and blows the chilled air into a room. The easiest next step is to place the human in this airstream and see if what we already have can be adjusted to specifically cool an adjacent human rather than the whole air in the space.

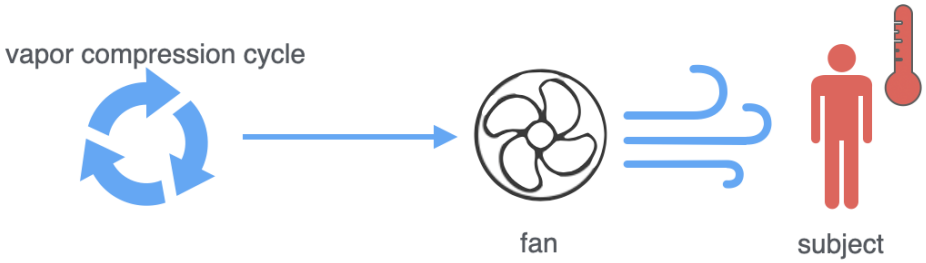

Figure 2-1: Human cooling strategy using status-quo technology. A vapor compression cycle cools air to be blown at a hot subject

Part 1: Defining System Requirements for Critical Cooling

This study is focused on a moment in time: peak indoor heat stress, occurring once in a 24-hour period, and the ability of a vapor-compression air conditioning system to remove heat from a human at that moment. As such, we will examine a case study and derive a cooling demand required by the human in that moment of time to maintain steady state. With no other sources of heat (e.g. cooking), a steady-state design targeted at this diurnal temperature peak will then be able to successfully remove energy from the human at all other times.

To establish the peak human thermal demand, we must parametrize the environment and the physiological human response. For the environment, data from Bardhan et al. 2024 will establish the geometrical and environmental conditions corresponding to peak indoor heat stress. This study quantified metrics during this peak heat stress moment for a traditional African settlement: It is understood that more extreme conditions can occur, but this case study serves as a starting point rooted in reality.

Table 2-1: Material Properties and Measured Temperatures for Traditional African Settlement
Emissivity Values Estimated from Literature

	Measured Peak Temperature (°C)	Material	Emissivity
Ceiling	55.4	Metal	0.9
Walls	33.7	Earth	0.9
Floor	26.2	Earth	0.9

Using these temperatures and the CBE Mean Radiant Temperature Tool (Center for the Built Environment 2025), MRT of 36C is calculated.

Table 2-2: Calculated Mean Radiant Temperature for Traditional African Settlement

Mean Radiant Temperature	36 °C

The air temperature in these homes varies with design. Bardhan et al. 2024 set 30°C as a threshold for high-risk heat stress and found the worst offenders had a high percentage of inside air at or above 30°C. Thus, we will assume 30°C for inside air. Typical peak annual air temperature and the corresponding relative humidity for the study location is shown in Table 2-3.

Table 2-3: Meteorological Data for Kisumu, Kenya
en.climate-data.org/africa/kenya/kisumu/kisumu-715071/

Peak Outside Air Temperature	36 °C
Avg High Relative Humidity	74 %

For the physiological human response, a human has six pathways to remove heat: radiation, convection, diffusion, respiration, conduction, and evaporation. In the critical cooling case study, we are designing for the most at risk humans: those who have impairments to the body's thermoregulation, specifically elderly with an attenuated sweating response (McKenna et al. 2023). While it is unclear how attenuated this response is, we will assume that the evaporative pathway is not available for heat transfer loss. A compromised evaporative pathway would also occur in environments of 100% relative humidity. Fanger 1972 established formulas for these pathways using a thermodynamic steady state model. These assumptions, equations, and the parameters in Table 2-1, Table 2-2, Table 2-3, and Table 2-4 result in the calculated values in Table 2-5.

Table 2-4: Physiological Parameters

Temperature of Exhaled Human Breath	36 °C	Mansour et al. 2020
Relative Humidity of Exhaled Human Breath	80 %	Mansour et al. 2020[1]
Skin Temperature of Heat Stressed Human[2]	35 °C	Winslow, Herrington, and Gagge 1937

Table 2-5: Calculated Heat Transfer From Human Body Inside Traditional African Settlement
Positive is Heat Leaving the Body

Breathing	+7.40 W
Radiation	-6.98 W
Conduction[3]	negligible
Diffusion[3]	negligible
Evaporative	0 W (compromised)
Convection	supplied by system

To solve for the resulting convective demand, we start by applying the first law of thermodynamics to the human body as a system, where there is no work done on the body or by the body:

$$\Delta E = Q \tag{1}$$

Where ΔE is the change in the amount of energy contained within the system during some time interval, and Q is the net amount of energy transferred in across the system boundary by heat transfer during the time interval. For an elderly human at rest, this change in internal energy is the enthalpy change across the system boundary, plus 72W of internal generation (Pannemans and Westerterp 1995):

$$\Delta E = \Delta H + Q_{gen} \tag{2}$$

[1] Mansour et al. 2020 found a large range of exhaled RH from 41%-91%, showing some dependency on room RH. 80% for this work is chosen as a guess where exhaled air is slightly more human than inhaled air.
2 Winslow, Herrington, and Gagge 1937 found that the evaporative heat loss pathway begins to dominate at a skin temperature of 35 °C. Since our design requires that the convective solution compensate for an attenuated evaporative pathway, we will set $T_s = 35\ °C$.
[3] Demonstrated by Wang et al. 2016. The conductive pathway could be an opportunity for heat transfer but would require a specifically designed system (e.g. liquid cooled jacket, evaluated later in the paper). In nominal life activities, conductive pathways are limited due to the small temperature deltas and limited contact areas that exist between human and objects at room temperature.

The enthalpy change is from three sources calculated above: enthalpy differences between inhaled and exhaled air, diffusion of water out of the skin (insensible perspiration), and evaporation of water from the skin (sensible perspiration).

$$\Delta H = breathing + diffusion + evaporation \quad (3)$$

Diffusion is assumed to be negligible, and evaporation is fully attenuated, such that the only enthalpy change is from breathing. Finally, our design criteria for critical cooling is that energy is leaving the system:

$$H_{in} - H_{out} + Q_{gen} - Q_{out} + Q_{in} < 0 \quad (4)$$

For this study the existence of this inequality regardless of the magnitude will be considered a successful design as the human system will not experience an increase in energy during the worst-case peak. As such the following limit will be solved for to find a power minimum for the design:

$$H_{in} - H_{out} + Q_{gen} - Q_{out} + Q_{in} = 0 \quad (5)$$

Specifically for this analysis:

$$-H_{breath} + Q_{gen} + Q_{rad} + Q_{conv} = 0 \quad (6)$$

Substituting values from Table 2-5:

$$-7.4 + 72 + 6.97 + Q_{conv} = 0 \quad (7)$$

$$Q_{conv} = -71.57\ watts$$

Thus, for this system to be effective, we need to convectively remove ~72 watts per human.

Finally, we aim to power this system with photovoltaic panels to enable grid independence. One 1.5 meter by 0.7 meter Renogy 200W solar panel will be used as reference for this study:

Table 2-6: Photovoltaic Data

Panel Size	1.5m x 0.7m
Rated Wattage	200
Typical Daily Watt-hours (20% efficiency)	1000
Panel Cost	$170

While batteries and other energy storage methods are possible to expand capability, the simplest system will be able to run on-demand where the solar panel is able to supply all the required

energy. As such, the panel above is rated for 80% output at 25 years. Conservatively, we should then design a system around 160W per panel.

Part 2: Equation development for convectively cooling a human using conditioned air

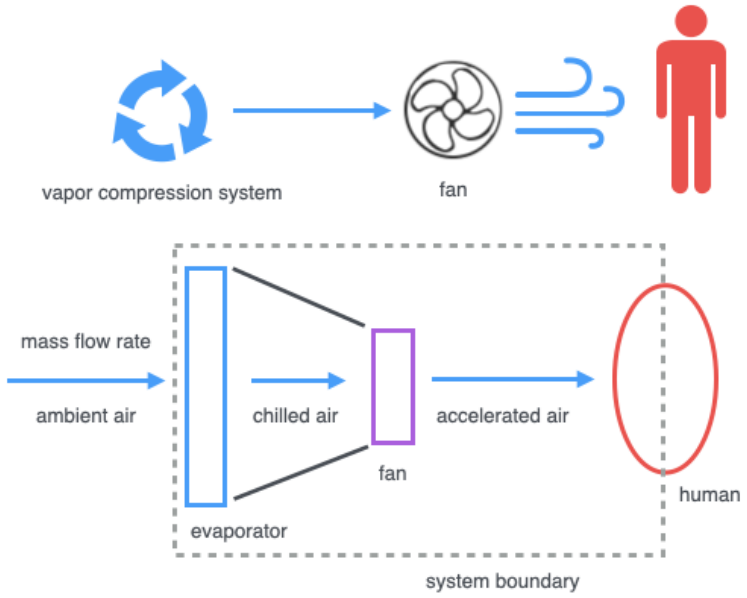

Figure 2-2: Thermodynamic system under review. Notice the single inlet, single outlet, constant ambient air temperature assumption inherent in the design.

Starting with Newton's Law of Cooling for convection, we can develop equations to define the design space that exists within 72 watts of convective cooling:

$$Q = A_{skin,cooled} * h * \Delta T \tag{6}$$

$$72 = A_{skin,cooled} * h * (T_{skin} - T_{air}) \tag{7}$$

Determination of h in terms of physical parameters:

Oliveira et al. 2014 established correlations for the convective heat transfer coefficient over a human as a function of air speed for each region of the body. The specific region of the body to cool in an extreme heat event is up for medical debate (Gaudio and Grissom 2016), however we will choose the chest as Winslow, Herrington, and Gagge 1937 found this to be the warmest area of the body during a heat event, thus improving convective heat transfer, and it is the largest area to convectively cool a human using a circular fan without complicated ducting.

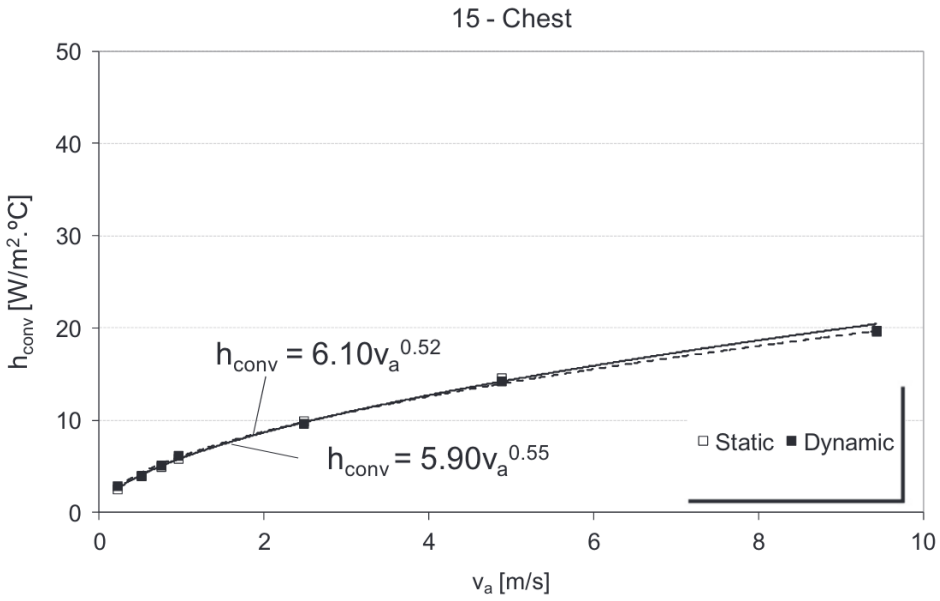

Figure 2-3: Empirical Correlation of Airspeed and Convective Heat Transfer Coefficient for the Human Chest *Oliveira et al. 2014*

Substituting this correlation, as well as the skin temperature from Table 2-4:

$$72 = A * 5.90v^{0.55}(35 - T_a) \tag{8}$$

We can visualize the relationship between A, v, and T_a:

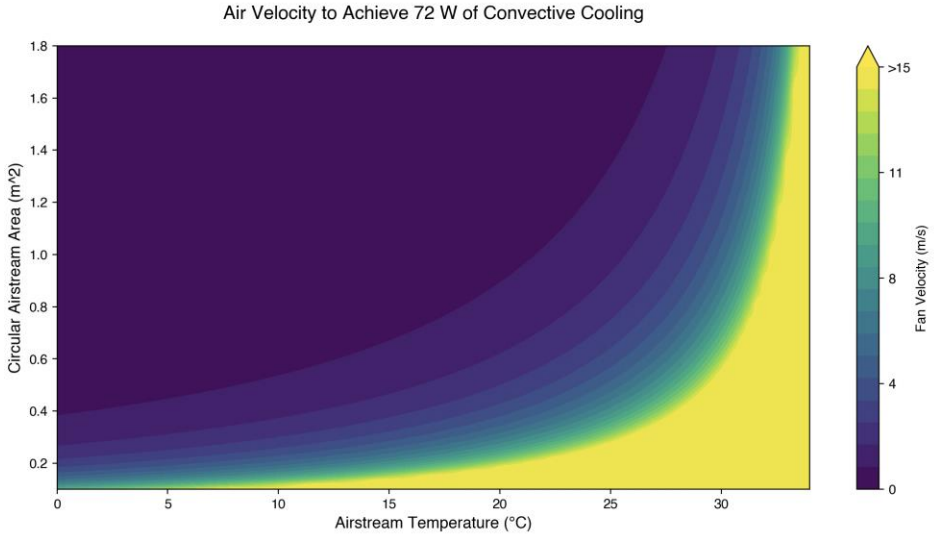

Figure 2-4: Computed air velocity as a function of airstream temperature and airstream area for convectively removing 72W. The upper bound of area is 1.8m^2, the skin surface area of an average human.

Using dimensional analysis, we can relate the power required for a fan to the airflow area and the airspeed:

$$Fan\ Power = f(\rho, D, V, \mu)$$

From this we find two non-dimensional groups:

1. Non-dimensional power: $\Pi_1 = {}^{P}/_{\rho D^2 V^3} = {}^{P}/_{\rho A V^3}$
2. Reynold's Number: $\Pi_2 = {}^{\rho DV}/_{\mu}$

It is expected from other fluid flow-power relationships that the non-dimensional power and Reynolds Number are related with a power law fit, where:

$${}^{P}/_{\rho A V^3} = k * {}^{\rho DV}/_{\mu}{}^{n} \tag{9}$$

Using a database of standard fans of different diameters covering our area bounds from mcmastercarr.com, the coefficients k and n can be found with a reasonable R^2:

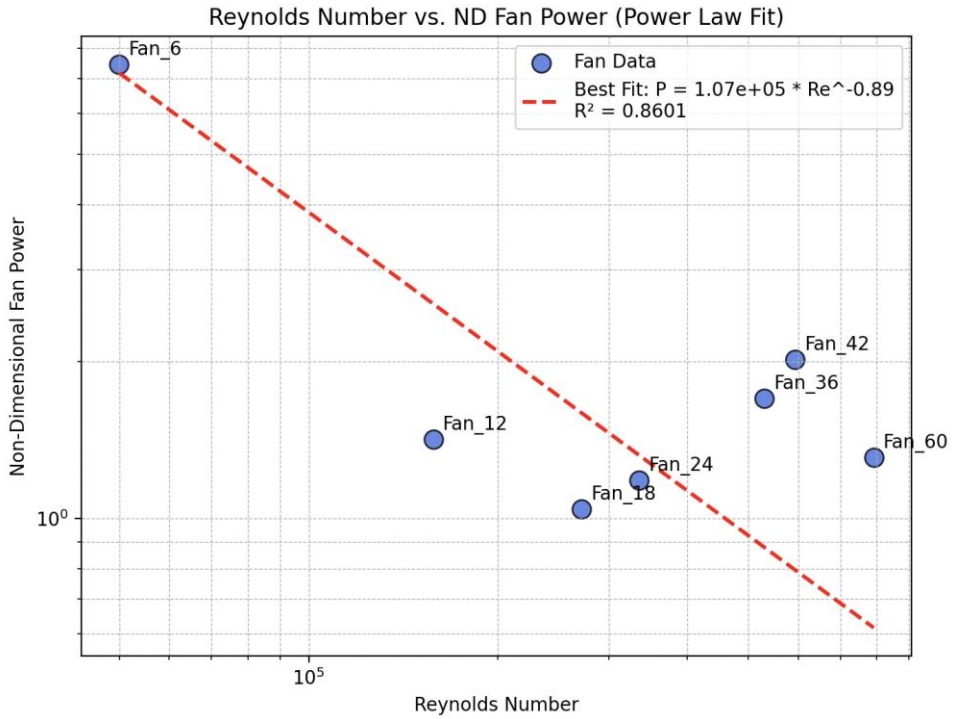

Figure 2-5: Power law fit of a known fan dataset to the related non-dimensional parameters

Rearranging to solve for V:

$$v = \left[\frac{P\mu^{-0.89}}{\rho^{0.11} A * 1.07 \times 10^5}\right]^{1/2.11} \tag{10}$$

Then plugging back into equation (8), we can rearrange to get the power as a function of air temperature and fan diameter. Assuming values for μ and ρ at 20 °C air temperature.

$$72 = A * 5.90 \left[\frac{P\mu^{-0.89}}{\rho^{0.11} A * 1.07 \times 10^5}\right]^{1/2.11}{}^{0.55} (35 - T_a) \quad (11)$$

Visualizing this:

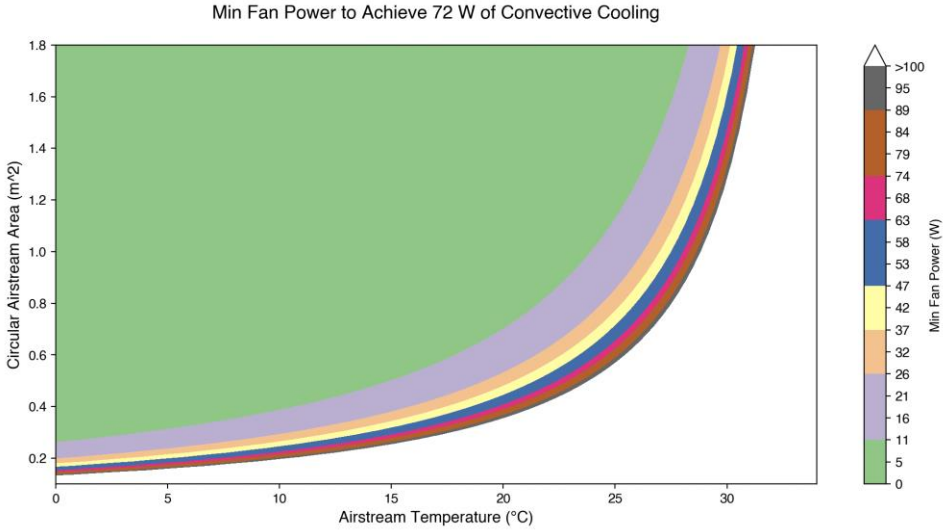

Figure 2-6: Computed fan power as a function of airstream temperature and airstream area for convectively removing 72W

From this chart, it's clear that a larger fan will often be preferred for a given airstream temperature from an energy reduction perspective. Mathematically:

$$\frac{\partial power}{\partial area} \ll \frac{\partial power}{\partial temp}$$

As such, we will define a max fan area of 0.28m^2, corresponding to a fan diameter of 0.6m, or twice the width of an average human chest. It is reasonable to expect that this area can be reduced to a human chest through a converging duct, allowing us to use the larger fan area for $A_{skin,cooled}$ in equation (7).

Part 3: Equation development for creating a low temperature airstream using a vapor compression cycle

The low air temperature supplied for this convective cooling will be a function of the vapor compression air conditioner design. We will make three assumptions for the system:

1) Both heat exchangers are optimally designed to move exactly the amount of heat to completely evaporate or condense the refrigerant. To phrase more technically, there is no superheat or subcooling in the system.
2) Pressure losses in the heat exchangers are negligible. Specifically, this pressure drop can be computed from the Darcy-Weisbach equation but requires system details beyond the scope of this paper (pipe diameter and Darcy friction factor).
3) No condensation occurs if the evaporator is below room dewpoint.

From a thermodynamics perspective, the power required to run a vapor compression system is that which drives an enthalpy change in the compressor:

$$\eta W_{compressor} = \dot{m}(h_{in} - h_{out}) \tag{12}$$

The enthalpy for a pure substance can be found using two other properties of state. For h_{in} we will use the fact that the refrigerant gas entering the compressor is fully saturated vapor at a fixed temperature of the evaporator (no sensible heating from assumption 1).

h_{out} is then established as the resulting state from multiplying a pressure ratio, pR, with the pressure corresponding to h_{in}, and assuming no change in entropy across the compressor. In reality, the entropy generated will increase the enthalpy by some amount. Since we are assuming that the condenser will always transfer enough heat to result in saturated liquid refrigerant, this increase in enthalpy only impacts compressor energy draw.

As such we will use η, or isentropic compressor efficiency, as the correction factor to get actual consumed power from the isentropic compressor assumption. According to Yahya 2011, for a relatively low-speed rotary compressor, η ~ 0.6:

$$0.6 * W_{compressor} = \dot{m} * (f(T_{evap}) - f(pR)) \tag{13}$$

While $f(T_{evap})$ is a tabulated dataset for a given substance, $\dot{m}$ and pR are a resultant from the specific compressor used. That being said, it is expected that $pR > 1$ as a resultant from compressing the gas, and $pR < 6$ as a general maximum capability for gas compressors (Giampaolo 2023). Similarly, $\dot{m}$ for a window AC system with a larger cooling demand is no more than 0.1 kg/s which will serve as an upper bound for analysis.

We can then plot this design space for a fixed T_{evap} across the possible $\dot{m}$ and pR ranges to visually understand the sensitivities of this power function. Also shown on this plot is a hypothetical compressor curve, demonstrating that a compressor will only be able to operate along some curve superimposed on this design space. It is important to note that most compressors cannot operate on the positive slope side of the curve due to surging (Yahya 2011).

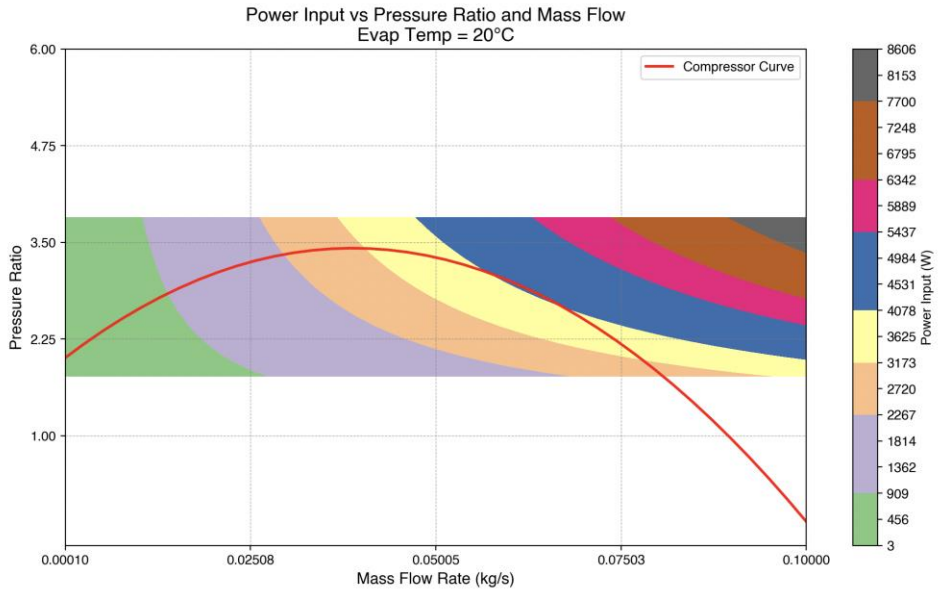

Figure 2-7: Power draw of a hypothetical vapor compression cycle across reasonable mass flow and pressure ratio ranges

Figure 2-7 shows that power is much more sensitive to mass flow rate than pressure ratio, so from a power-minimization perspective we should be minimizing mass flow rate while allowing pressure ratio to be a resultant of the compressor design and condenser requirements.

Determination of mass flow rate and pressure ratio

This relationship between mass flow rate and pressure ratio is critical to the power function but traditionally requires higher fidelity system design than desired for this study.

Canova et al. 2015 and Yang 2022 experience a similar problem with automotive turbochargers, where a design space for optimization is desired, but information is not readily available to map the design space. We will follow a similar, but simplified approach, where non-dimensional parameters are determined from a known compressor and then the non-dimensional parameters are scaled to reasonable values.

For a compressor, the non-dimensional relationship is given by Canova et al. 2015 and corroborated by Yahya 2011.

$$\frac{p_{01}}{p_{02}}, P, \eta = f\left(N, D, \frac{s}{l}, \frac{h}{l}, \dot{m}, \rho_{01}, \mu, \gamma, a_{01}\right) \tag{14}$$

Notion is defined in Yahya 2011.

We will focus on the following Π-group to understand the opportunity for changes in mass flow rate by reducing the diameter of the compressor:

$$\Pi = \left(\frac{\dot{m}\sqrt{RT_{01}}}{p_{01}D^2}\right)\left(\frac{a_{01}}{ND}\right)\left(\frac{1}{\sqrt{\gamma}}\right) \tag{15}$$

Table 2-7: Notation for Non-Dimensional Rotary Compressor Relationships

$\dot{m}$	mass flow rate of gas
R	gas constant
T_{01}	gas temperature at compressor entrance
a_{01}	elasticity of gas, accounted for as the velocity of sound at compressor entrance ($a_{01} = \sqrt{\gamma RT_{01}}$)
p_{01}	gas pressure at compressor entrance
γ	ratio of specific heats ($^{C_p}/_{C_v}$)
N	rotational speed of compressor
D	rotor diameter

The following results from using this Π-group:

$$\dot{m}_{new} = \left[\frac{\dot{m}T_{01}}{p_{01}D^3N}\right]_{existing} \times \left[\frac{p_{01}D^3N}{T_{01}}\right]_{new} \tag{16}$$

Table 2-8: Scaled Mass Flow Rate

	Diameter (m)	Mass Flow Rate (kg/s)
Existing compressor	0.240	0.0395
Minimized compressor	0.030[4]	dynamically computed

The final value to find output power from Figure 2-7 is the pressure ratio. While this is a function of how the system places load on the compressor, the pressure ratio's sole thermodynamic job is to raise the temperature of the refrigerant above ambient such that full condensation would occur when exposed to outdoor air in the condenser. To limit the scope of this paper, it is assumed that the outside heat exchanger is designed for full condensation when the condenser temperature is no less than 5 degrees above ambient temperature. Using values

[4] The assumption here is that it is feasible to scale a compressor to a 30mm diameter without breaking similitude. This is the most aggressive assumption in this paper. However, Aspen Compressors sells compressors with diameters down to 50mm. 30mm is arbitrarily chosen, but due to the importance of mass flow rate in the energy calculation, it seems reasonable that the directionality of this paper is valid even down to a 30mm diameter.

from part 1, this means that the condenser will at minimum need to be 41 °C to consider the computed power valid. More specifically, the pressure in the condenser is that at 41 °C saturation temperature, while the pressure in the evaporator is that at the listed evaporator temperature. This results in the chart shown in Figure 2-8, demonstrating power values for a low mass flow rate compressor design across pressure ratios that result in acceptable condenser temperatures. The bottom edge of this chart corresponds to 41 °C condenser saturation temperature, while the top edge is the highest saturation temperature in the lookup table (78 °C). An actual system will then land along the Y-axis is a function of the ΔT required for complete condensation in the condenser. With optimal condenser design the system will require a smaller ΔT and move towards the bottom of the chart. If the condenser design is compromised, a larger ΔT is needed for complete condensation and the design point will move towards the top of the chart.

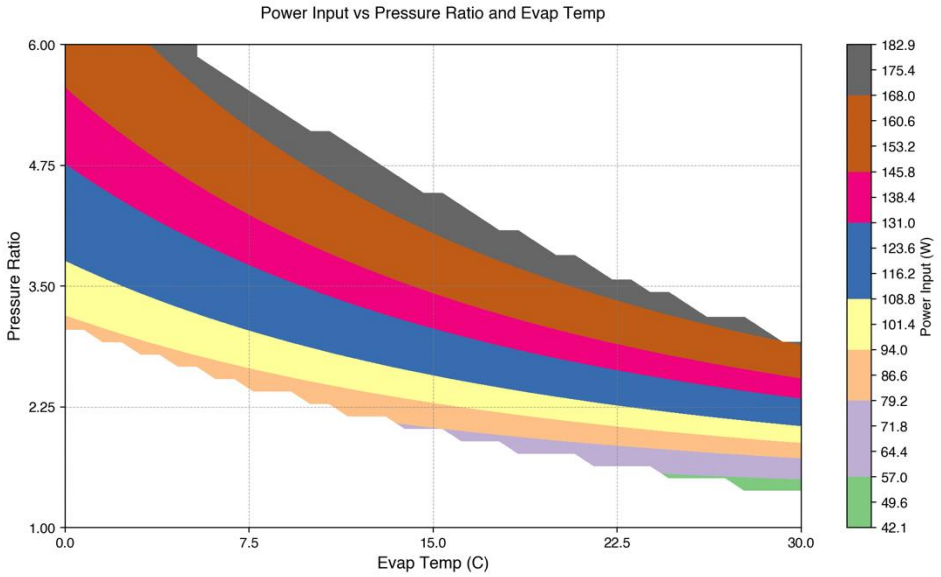

Figure 2-8: Power draw of a vapor compression cycle across evaporator temperatures after mass flow rate is solved

From Figure 2-8, we can see for the small mass flow rate from a mini compressor the theoretical power input ranges between 42.1 and 94.0 W dependent on the desired evaporator temperature and if the condenser can operate with $\Delta T = 5$.

Part 4: Relating T_{evap} and $T_{airstream}$

The final link between Figure 2-6 and Figure 2-8 is to develop a relationship between the evaporator temperature achieved by the vapor compression cycle and the airstream temperature after the air has blown over the evaporator heat exchanger. Again, we are assuming no condensation on the evaporator if below room dew point.

For the evaporator, the heat transferred out of the refrigerant must be equal to the heat transferred into the air from conservation of energy.

$$Q_{ref} = Q_{air} \tag{17}$$

Then, from conservation of mass, the air mass flow rate into the system must be the same as that leaving the system:

$$\dot{m}_{in} = \dot{m}_{out} \tag{18}$$

It can be shown that the density change as the air cools will be negligible at constant atmospheric pressure:

Table 2-9: Air Density Change from 0°C to 30°C

Air Density at 30 °C	$1.164\ {}^{kg}/_{m^3}$
Air Density at 0 °C	$1.292\ {}^{kg}/_{m^3}$

Part 2 established a relationship between 72 watts of convective cooling, air velocity, and air temp, shown again in Figure 2-9:

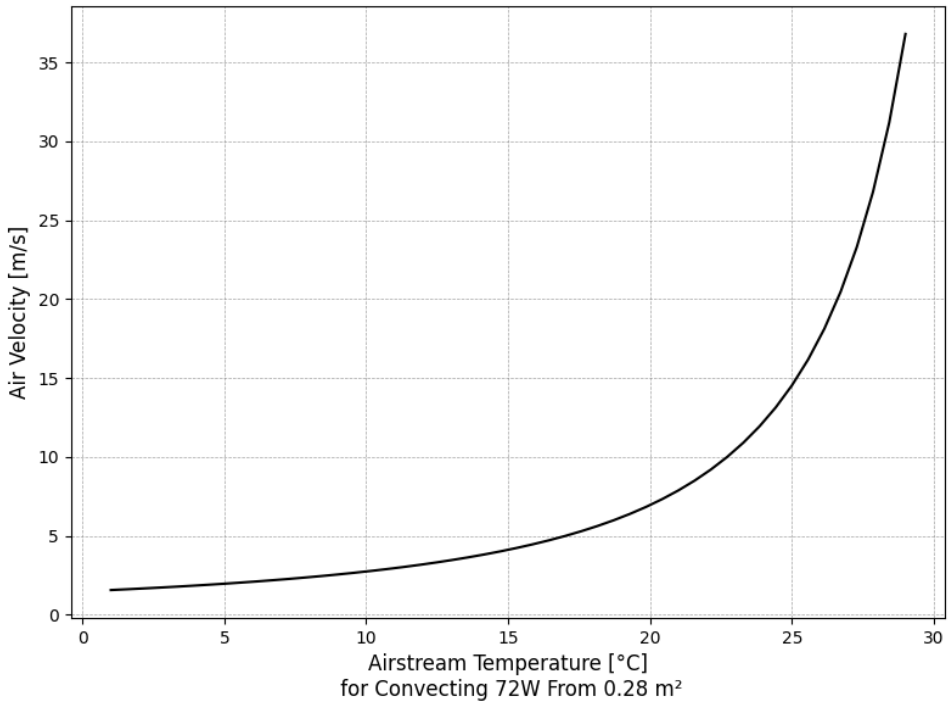

Figure 2-9: Minimum airspeed and temperature needed to convectively cool a human using a fan diameter approximately double the width of a human torso

We can then compute for each airstream temperature the resulting mass flow rate, then use the following equation to determine the amount of heat that needs to be transferred into the air to lower the 30 °C ambient air to that airstream temperature at that mass flow rate:

$$Q = \dot{m}_{air} C_{p,air} \Delta T_{air} \tag{19}$$

Plotting this required Q as a function of $T_{air,cooled} = (30 - \Delta T_{air})$ we see exceptionally large power values relative to current air conditioning systems.

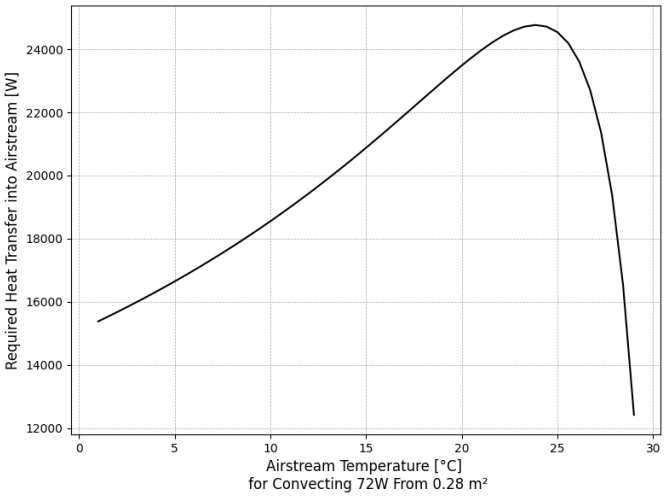

Figure 2-10: Required heat transfer into air at the mass flow rates needed to convectively cool a human

Looking then at maximizing the area for convective cooling to the upper limit of skin surface area, the heat transfer required is still on the same order of existing AC systems:

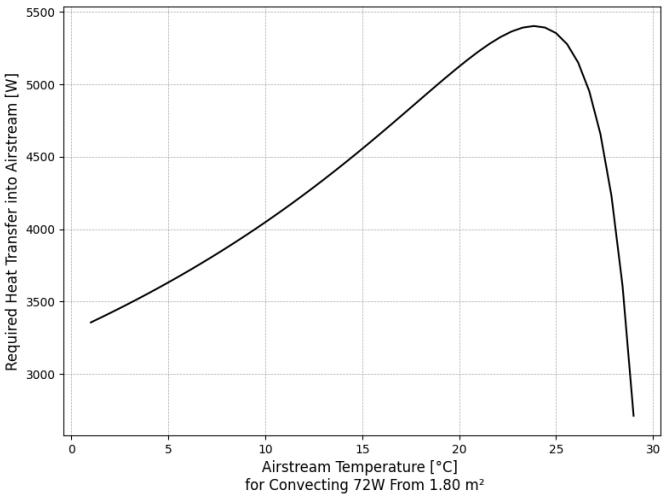

Figure 2-11: Required heat transfer into air at the mass flow rates needed to convectively cool a human over a maximized surface area

As such, Figure 2-11 proves even with the many conservative assumptions made in Part 1 through 3, it is not possible to immediately apply in a heat stress situation a convective cooling solution that uses any less energy than existing systems.

Fundamentally, this result is because existing vapor compression air conditioning systems do not convectively cool a human to steady-state as shown in Figure 2-2. Instead, vapor compression air conditioners rely on circulation of a fixed volume of air, slowly lowering the temperature of the air a few degrees at a time. In turn, this reduces the ambient air temperature, as well as lowers the mean radiant temperature by lowering the temperature of the room surfaces. Natural convection, a lower mean radiant temperature, and a greater enthalpy loss from breathing all contribute to thermal equilibrium in this case. Attempts to increase this rate of heat transfer out of air require significant power to aggressively change the sensible temperature of air as shown but also begin to lower the air temperature to dew point where energy goes towards condensing water out of the air and not lowering its sensible temperature.

Lastly, it is important to note that the heat transfer coefficient correlation in Figure 2-3 is not valid across all simulated air velocities. In fact, at low air velocities this heat transfer correlation should flatline where natural convection takes over.

As such, there are two more investigations required to complete the evaluation of vapor compression air conditioning: 1) energy usage over a full day from recirculating a fixed volume of air and 2) air mass flow rate minimization to more accurately capture the effects from natural convection not captured in Figure 2-3 at low air velocities.

Part 5: Examining air recirculation

We will quantify the energy usage from recirculating air over time not in efforts to find minimization, given the previously shown fundamental infeasibility of moment-in-time convective cooling, but as a baseline for comparison to other, more energy efficient systems.

The existing structures studied in Bardhan et al. 2024 are naturally ventilated with no efforts to air seal or insulate.

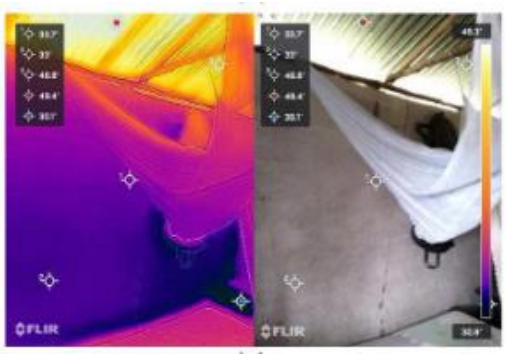

Figure 2-12: Screenshot from Bardhan et al. 2024 showing home construction

Using *ClimateStudio* (Solemma 2025) a simulation of the building in Part 1 was created with the parameters shown in Table 2-10:

Table 2-10: ClimateStudio Simulation Parameters

Wall R-Value (m^2K/W)	2.3	Rammed earth
Wall Capacitance ($kJ/K/m^2$)	472	
Ceiling R-Value (m^2K/W)	0	Corrugated steel
Ceiling Capacitance ($kJ/K/m^2$)	4	
Air changes per hour	2	*Estimated*

These values are estimated. To validate these estimations, the simulation is run without any active cooling. We then expect to see internal air temperatures and MRT on par with those measured in the study:

Table 2-11: Validation of ClimateStudio Model

	MRT	Peak Inside Air Temp
Study	36 ℃	30-35 ℃
Simulation	35 ℃	34 ℃

Adding in active cooling, the following kWh input is determined assuming a cooling COP of 3.

Table 2-12: ClimateStudio Peak Day Simulation Results

Internal Air Setpoint	Peak Daily kWh Power Draw
26 ℃	2.23 kWh
22 ℃	5.33 kWh

More importantly, the peak demand for the active cooling scenario:

Table 2-13: ClimateStudio Peak Power Draw Simulation Results

Internal Air Setpoint	Peak W cooling load	Peak W power draw (COP = 3)
26 ℃	2000 W	667
22 ℃	3000 W	1000

For the 26 ℃ case we would require an AC with at least 6800 BTU/h capacity and for the 22 ℃ case we would require an AC with at least 10,200 BTU/h capacity, to put these in terms used in AC marketing.

Figure 2-13: Sample Window Air-Conditioners

Left: 26 ℃ case: 8000 BTU/h AC drawing ~700W, $254
Right: 22 ℃ case 12000 BTU/h AC drawing ~1000W, $350
Chosen BTU/h values are rounded up from computed values, as only certain values are sold
Images and data from homedepot.com

While it is possible to run these systems from solar panels, it requires significant capacity to handle the peak loads. The 700 W system would need a minimum of 5 panels described in part 1 at a cost of $800, in addition to the equipment to connect the system together.

Finally, if natural convection is not enough in these cases to maintain equilibrium, a fan will be required remove the 72W from the human chest. In this situation, we require relatively high airspeeds given the heat transfer correlation in Figure 2-2. Even with a maximized cooled area, the fan power will add 10-30% to the overall power budget.

Table 2-14: Fan Power Requirements for Convective Cooling

Internal Air Temperature	Fan Power for Convectively Cooling Over Chest (0.5 m^2 cooled area)
26 °C	232 W
22 °C	56 W

Part 6: Mass flow rate minimization

As previously discussed, the analysis thus far does not account for natural convection coefficients and low mass flow rate air conditioner systems. This option could extend the time for heat transfer at both the evaporator and the human while eliminating meaningful fan power draw.

From a general analysis of internal flow with constant wall temperature, a time constant for the change in fluid temperature is shown:

$$\tau = \frac{\dot{m}c_p}{hPL} \tag{20}$$

Where a larger time constant is a smaller change in temperature over length L and a smaller time constant is a larger change in temperature over length L.

This establishes the idea that for internal flow minimizing mass flow rate over a surface of constant temperature will increase the change in temperature experienced by a fluid flowing over a fixed distance. As long as the heat transfer coefficient does not scale with mass flow rate (as was the case for our high power design in Figure 2-10), minimizing mass flow rate will cause a larger change in temperature.

A reasonable starting point to evaluate a low mass flow rate design would be natural convection around the human following the direction of air as it moves due to warming: toes to head. We could place a human on top of an evaporator, supply a small initial flow rate upwards, and allow natural convection to carry the air upward.

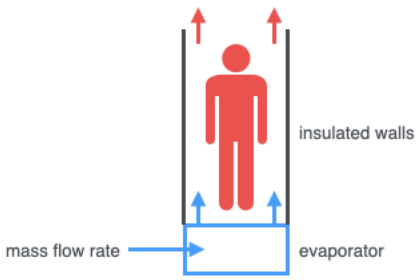

Figure 2-14: Model for low mass flow rate design

From an energy balance across the evaporator, assuming 160W available from a solar panel and a vapor compression COP of 3, to deliver 25 ℃ air from 30 ℃ ambient:

$$Q = \dot{m} c_p \Delta T \tag{21}$$

$$480 = \dot{m} * 1005 * 5$$

$$\dot{m} = 0.096\ kg/s$$

Then, for a single stream energy balance using this mass flow rate over the human shown in Figure 2-14:

$$Q = \dot{m} c_p \Delta T \tag{22}$$

$$72 = 0.096 * 1005 * \Delta T$$

$$\Delta T = 0.75\ C$$

If we can show that a human can warm a 25 ℃ stream to at least 25.75 ℃ through natural convection, then this system is feasible.

The situation of a human with constant skin temperature heating up a colder fluid moving past them is similar in nature to internal pipe flow, where there is an exponential decay of fluid temperature along the length of flow.

$$\frac{T_{skin} - T_{air,out}}{T_{skin} - T_{air,in}} = e^{\left(-\frac{PLh}{\dot{m} c_p}\right)} \tag{23}$$

Oliveira et al. 2014 compiled natural heat transfer coefficients for humans in the range of 3-5 W/m^{2}K.

Substituting the skin surface area for the pipe surface area PL, we can compute $T_{air,out}$ using the upper bound of h:

$$T_{air,out} = T_{skin} - \left(T_{skin} - T_{air,in}\right)e^{\left(-\frac{PLh}{\dot{m}c_p}\right)}$$

$$T_{air,out} = 35 - (35 - 25)e^{\left(-\frac{1.8*5}{0.096*1005}\right)}$$

$$T_{air,out} = 26.7\ C$$

As such, the $\dot{m}$ for this situation agrees with the empirical convective heat transfer correlation and this device seems plausible to operate off a single solar panel.

However, it is important to note that high humidity in the room may cause the dew point to exceed the evaporator temperature. As such, energy draw will be higher in this case as some of the evaporator cooling power will go towards dehumidification.

Chapter 3 - Discussion of Alternatives

The idea of cooling humans is not a new one, as such there is a significant body of work examining the options.

Epstein, Shapiro, and Brill 1986 compared different human cooling devices: a water-cooled vest, a water-cooled hood, an air-cooled vest, an air-cooled hood, an ice bag vest, and "zone cooling". Zone cooling is a similar strategy originally explored in this paper, where cool air supplied by an air conditioner is directed at the human using a fan.

Using our 72 watt design criteria, only two of the technologies could meet this cooling capacity from empirical testing: ice bags and a water cooled vest. This corroborates the work in parts 2-6, where the challenges of convective cooling are demonstrated. Examining these two technologies in detail:

Ice or Phase-Change Vest (Solid-State Cooling):

Ice bags or phase-change materials do not constitute on-demand cooling as they need to be cooled prior to use. From an energy use perspective, these would work in conjunction with a solar powered refrigeration device. However, from a usability perspective it is a significant compromise in our use case to require pre-planning. Finally, from an physiology standpoint, Gao, Kuklane, and Holmér 2011 found no reduction of rectal temperature (a common analog for core temperature), from a cooling vest, so direct use-case testing is needed to understand if these can help effectively prevent heat stroke in a human.

All these solid-state vest designs also suffer from unmitigated heat losses to the environment, while having an additional limitation of high thermal contact resistance between the human and the vest. At the extreme, a scenario could exist in which the thermal path of least resistance to melt the working material is that between the vest and the environment, and not the vest and the human. In fact, Epstein, Shapiro, and Brill 1986 did not account for environmental losses when calculating the cooling power of a vest, instead computing the capability of a cooling vest to cool everything it touches. In practice, this could be addressed by wearing a winter parka over the vest.

The cooling capacity of the ice bag vest was estimated from the amount of ice melted as follows:

$$C_c(\text{ice}) = 79{\cdot}71 \times 69{\cdot}8 \times W/60 \quad (W)$$

where: 79·71 is the heat of fusion of water (kcal kg^{-1}); 69·8 the conversion factor from kcal min^{-1} to watts, W/60 is the rate of ice melting (kg min^{-1}).

Figure 3-1: Screenshot from Epstein, Shapiro, and Brill 1986 showing their calculation of cooling power of an ice vest.

The implicit assumption they made is that the incoming energy to melt ice comes from the body alone. The relatively hot 50 °C air during the test must have provided some if not much of this energy.

Figure 3-2: Various cooling vests for sale on uline.com
Prices (L to R) are $46, $170, $190, $200

Circulating Liquid Vest or Chair:

Figure 3-3: Commercially available Personal Cooling Systems

Left: Liquid Cooled Chair Insert from Polar Products
Right: BCS-4 Body Cooling System for Bomb Disposal Suits

Liquid cooling systems exist in a wide range of commercial applications, often under the generic title of Personal Cooling Systems (PCS). Figure 3-3 shows currently available systems for either generic use or specific occupations.

Jette et al. 2004 tested available PCS on a thermal manikin, following similar logic to ASTM 2003 and ISO 2001 for testing these devices. They calculated for a manikin temperature of 34°C

an effective cooling of ~70W using 7.28 ℃ water. This system drew ~90W for the chiller with a COP of 3. These numbers for both heat removal and power required show potential for critical cooling. However, a custom chiller design is needed to enable operation during a heat event and may increase power draw due to the warmer condenser temperatures needed. The study here operated the chiller in 23.5 ℃ ambient air, so unless the condenser is extremely oversized a new design is needed.

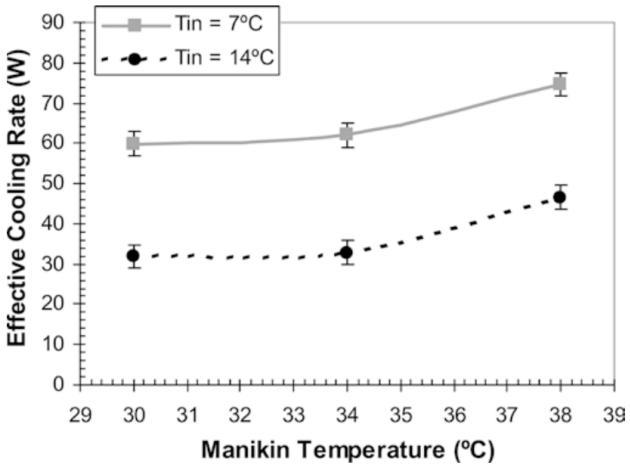

Figure 3-4: Effective cooling rate calculated by Jette et al. 2004 for a commercially available cooling vest

Evaporation:

Lastly, it is important to acknowledge that the default technology employed by the human body is evaporative cooling. The use case developed in Part 1 is one where sweat evaporation is compromised due to age or environment, but that does not prevent use of a system designed to deposit water and provide dry air around a human to promote artificial evaporative cooling. At its simplest level this is a spray bottle with a fan in a dry environment.

Combining the evaporative heat loss equation from Fanger 1972 with the fan power from Part 2, the following chart is produced for our 72W design specification:

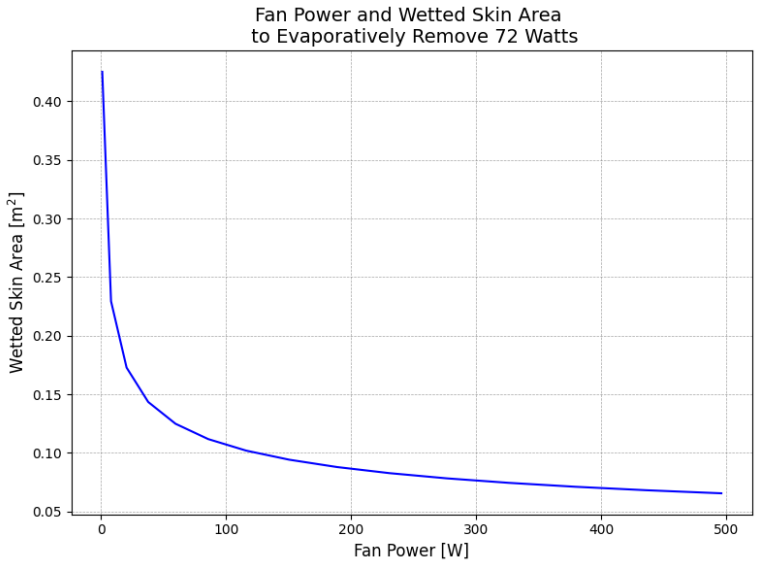

Figure 3-5: Fan power to evaporatively remove 72W from different wetted areas of skin. Plot is showing 30 ℃ air with 25% RH

From Figure 3-5 it seems plausible that a solar powered fan can evaporatively cool a human with small, wetted areas. However, this device would require additional power to create dry air, likely significantly more energy than the fan power. In an environment where the air is naturally dry, this strategy will be the most effective of all, but this solution lacks the resilience to extreme environments, such as high humidity, required of critical cooling technology.

Radiation:

From Part 1, we see that radiation effects are important enough to include in the overall energy balance of a human at rest. In fact, the human is also the most sensitive to the radiation parameters. Adjusting the mean radiant temperature of the room, or the human skin, has an outsized impact on the heat transfer requirements of the human compared to the other environmental variables. At a first order, insulating the roof or strategic ventilation could reduce the surface temperature of the ceiling and provide significant reduction in room MRT and thus the amount of excess heat removal required for homeostasis.

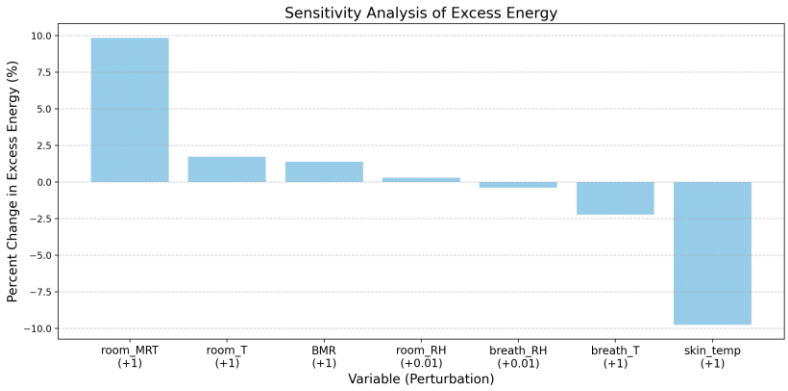

Figure 3-6: Sensitivity analysis of the excess energy generated by the human showing high sensitivity to the variables in the radiation calculation

This is expected as temperature is raised to the fourth power in radiative heat transfer, while the other parameters do not scale in the same way. Those first order suggestions to change the temperature of the ceiling could reduce the required heat transfer by 10%. Taking this a step further, it is worth exploring the energy required to run a system in which the direction of radiative heat transfer can reverse and remove heat from the human.

Looking at the most basic radiative heat transfer situation: a black body in a large, black enclosure, Figure 3-7 demonstrates that up to ~500W/m^2 can be radiatively transferred from a surface temperature of 35 °C (e.g. skin). This human-scale problem is convenient in that radiation can mathematically account for all the heat transfer from a human. Also marked on Figure 3-7 is the black body heat transfer between a 35 °C surface and a 1 °C surface, showing that 191W/m^2 could be transferred between human skin and a 1 °C blackbody enclosure, such as walls chilled to a reasonable minimum water temperature.

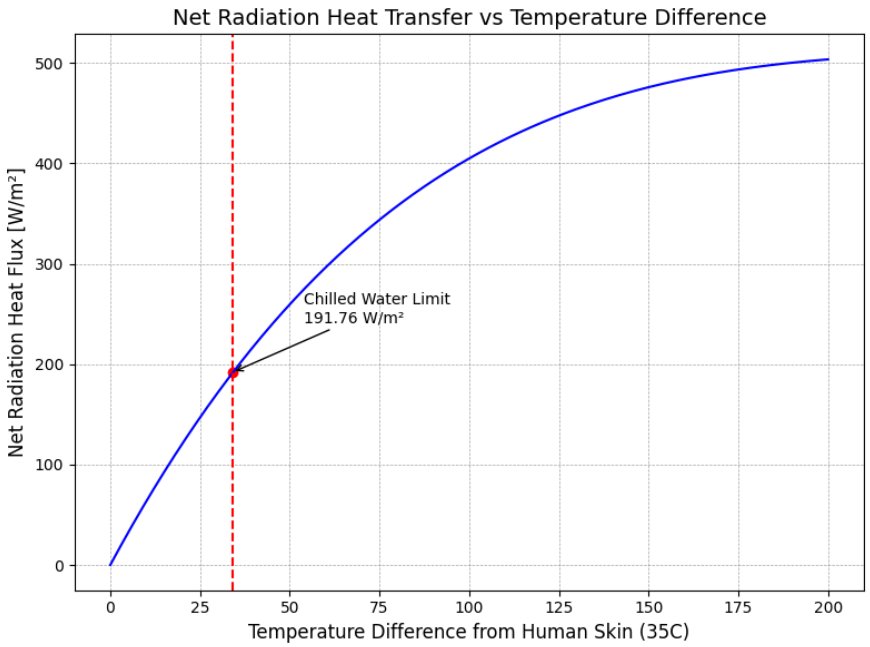

Figure 3-7: Net radiative heat transfer between a black body in a large black enclosure

This simple example is what would occur for a human in a large room with walls, floor, and ceiling held at 1 °C. It is easy to see that the energy requirements, let alone practicality, for this example are a non-starter for a low-energy solution, as cooling the walls would require also accounting for the cooling demand from the sun, the warm ambient air, and the condensation energy from holding a surface well below dew point.

Instead, we can look to a general radiation equation to understand what variables are important. For two surfaces that exchange radiation with each other, the net radiative heat transfer is:

$$Q_{net,1-2} = \frac{\sigma({T_1}^4 - {T_2}^4)}{\left(\frac{1-\varepsilon}{\varepsilon A}\right)_1 + \left(\frac{1}{A_1 F_{1-2}}\right) + \left(\frac{1-\varepsilon}{\varepsilon A}\right)_2} \quad (24)$$

Where ε is the emissivity of the surface, F_{1-2} is the view factor between surface 1 and 2, A is the surface area of each object, T is the temperature of the surface in Kelvin, and σ is the Stephan-Boltzmann constant. Equation (24) is based on the idea of a resistive radiative network, where surfaces and space have resistance to radiative heat transfer. A successful radiative design will minimize the resistances to move as close as possible to the black body ideal in Figure 3-7. As such, we want to maximize F_{1-2}, or the fraction of energy leaving our cold source and intercepting our human, maximize the surface area of cold source and human, and maximize emissivities for the surfaces.

In addition to these variables, an ideal radiative solution would be isolated from losing energy to other forms of heat transfer: conduction, convection, and condensation, as well as radiation from the warmer room.

Vacuum insulation presents one option that can insulate against conduction, convection, and condensation, while allowing radiation to pass depending on the materials. From a structural stability perspective, a cylinder is a good starting point to evenly distribute any pressure differences and is the standard shape for vacuum insulated hardware. This design is shown in Figure 3-8. Most critically, this design requires an outer material that is strong enough to support the pressure differential from vacuum on one side, while also allowing transmission of far-infrared radiation (3-to-75-micron wavelength range). Glass or acrylic is a good choice for structural strength but has no IR transmittance in this range. It is unclear if such a material exists but will be assumed to exist with 100% transmissivity for this exercise.

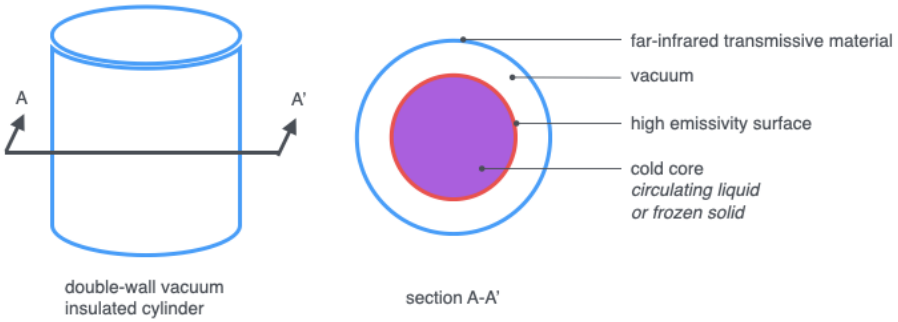

Figure 3-8: Schematic of radiative cooling cylinder

Lastly, attempts must be made to maximize the view factor between this cylinder and the human, while also lowering the view factor between the cylinder and the rest of the room. At an extreme, the human and cylinder could be placed in a reflecting enclosure, where all the radiation must enter or leave the human or cylinder. This complicates the use case for this design, which has potential be differentiated from liquid cooling solutions by not requiring a special interface or enclosure.

Instead, we can assume the cylinder has specular reflectors built in to improve view factor between the human and the cylinder and shield from the room. A top-down schematic of this configuration is shown in Figure 3-9.

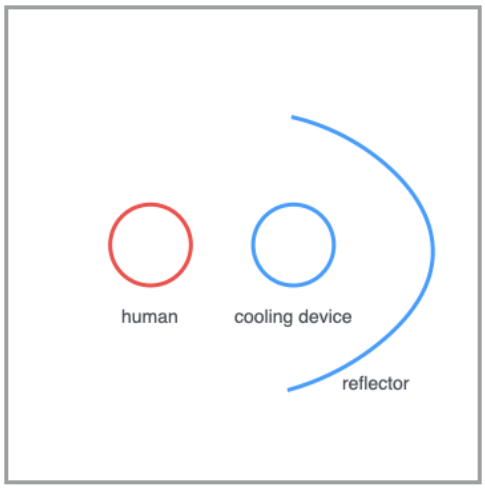

Figure 3-9: Top-down view of cooling device with reflectors to increase view factor

To understand the radiative exchange of this system, we need to calculate the three-body interaction between the human, cooling device, and room. First, the view factors must be determined.

View factor between human and cooling device:

If we assume the reflector is designed to connect lines of sight from the front of a human to the cooling device, an estimate for view factor is just less than half of the total human radiosity. Phrased differently, it would be challenging to capture anything more than half of the radiation from one side of a human:

$$F_{12} = 0.45 \tag{25}$$

View factor between human and room:

From the summation rule:

$$1 = F_{11} + F_{12} + F_{13} \tag{26}$$

Since the human is modeled as a cylinder here, it does not view itself, so $F_{11} = 0$

$$\text{Then } F_{13} = 0.55 \tag{27}$$

View factor between cooling device and room:

From the reciprocity rule:

$$A_1 F_{12} = A_2 F_{21} \tag{28}$$

$$F_{21} = \frac{A_1}{A_2} F_{12} = \frac{1.6}{1.0} * 0.45 = 0.72 \quad (29)$$

From the summation rule:

$$1 = F_{21} + F_{22} + F_{23} \quad (30)$$

The cooling cylinder will view itself from the reflector, so we will estimate $F_{22} = 0.05$ (31)

$$\text{Then } F_{23} = 0.23 \quad (32)$$

Table 3-1: Parameters for three-body radiative exchange

F_{12}	0.45	View factor between human and cooling device
F_{13}	0.55	View factor between human and room
F_{21}	0.72	View factor between cooling device and human
F_{23}	0.23	View factor between cooling device and room
A_1	1.6m^2	Surface area of human, not accounting for bottom of feet
A_2	1.0m^2	Surface area of cooling device
ε_1	0.98	Emissivity of human skin
ε_2	0.95	Emissivity of cooling device surface

Since the human is smaller than the room, and the room walls have high emissivity (>0.95) we will claim the room behaves as a blackbody. Human skin and the cooling device surface also have high emissivity, so we will treat them as blackbodies as well.

For simplicity we will also linearize radiation around 291.65 K (halfway between 1℃ and 36℃), giving a radiative heat transfer coefficient of:

$$h_r = 4\sigma {T_{ref}}^3 = 5.63 \ {}^{W}/_{m^2K} \quad (33)$$

Computing the three radiative heat exchanges:

$$q_{hu \to cool} = h_r A_1 F_{12} \Delta T = 137.8 \, W \quad (34)$$

$$q_{cool \to room} = h_r A_2 F_{23} \Delta T = -45.3 \, W \quad (35)$$

$$q_{hu \to room} = h_r A_1 F_{13} \Delta T = -4.95 \, W \quad (36)$$

Computing the natural convection that would remove additional heat from the human, using the lower bound of natural convection heat transfer coefficient for a human:

$$q_{ambient \to hu} = h A_{hu} \Delta T = 3 * 1.8 * -5 = -27 \, W \quad (37)$$

Hence, the net heat transfer rate from the human is 160W, above our 72W design criteria, and the rate into the cooling device is 183W.

The cooling device then needs a chiller with a cooling capacity of at least 183W with ~1°C water. Figure 3-10 shows a commercially available chiller with that capacity that can continuously operate off a single 160W solar panel:

Figure 3-10: Candidate chiller from RigidHVAC.com

The working fluid for this concept could even be subzero liquids, such as liquid nitrogen at ~70 K, or even frozen liquids. For example, a block of ice in the same size used for this study has enough energy to last 21 hours with -183W heat transfer. However, using subzero liquids or forming ice in this system will take more energy due to a lower chiller COP at these temperatures, as well as increased reliability concerns with an ice-forming device.

Figure 3-11: Hypothetical implementation of radiative cooling device (generated with ChatGPT). Reflectors would need to be significantly larger than shown to achieve a view factor of 0.72

Chapter 4 – Discussion

It is clear from this work that redesign of our status-quo cooling solution will not enable a reduced energy or grid-independent cooled world. At large scale vapor compression air conditioning can effectively keep many people cool at once, such as in centralized cooling centers, but it will not serve the needs of an individual at risk in their own home without access to a reliable energy grid.

Ironically, this work has shown that existing vapor compression systems are an *efficient* way to cool air. The fact that a device can move more heat than energy consumed is just short of magical. This technology could have an important role in an energy minimized future, but only if we took care to maintain the temperature of the treated air with properly air sealed and insulated buildings, as well as developing a central electricity grid resilient to heat events.

The reality is that we may never achieve these two goals, let alone on the aggressive timeline dictated by climate change. The situation then demands that we focus in parallel on developing on-demand, off-grid, use case specific solutions to keeping people cool. Many technologies, or combination of technologies, can be competitive in this use case but three stand out as having a path towards appropriate energy draw, low-cost manufacturing, off-grid capability, and fast (years or less) development time:

1) Low mass flow rate air conditioning leveraging natural convection
2) Circulating liquid cooling devices
3) Radiative cooling devices

The work shown for these three technologies demonstrates that finding solutions to keep humans cool across the world is not impossible: except for the strong, far-IR transmissive surface required for the radiative cooling cylinder, we have all the technology to develop these systems today. Although further work is needed before any of these can save lives, they are mature enough that the remaining challenges are not about discovering unknown problems, but about solving well-understood ones common to all technology. Specifically, liquid cooling devices, which are already on the market, need integration into a solar focused system along with design for usability such that they can be deployed quickly in an emergency. Research continues to be conducted on these systems, but it seems that they are mature enough to require implementation, not research. With some work here, these systems could be deployed nearly immediately.

Of all the technologies, radiative cooling has the least amount of research and thus requires more effort to bring to the same technology readiness level as (1) and (2). It is clear from this work that radiative cooling can theoretically keep a human cool, it's just a question of what kind of tradeoffs are required, such as requiring the human to be enclosed and shielded from the room.

This system is also extremely sensitive to the environment and the ability to direct the radiation which will require careful user design relative to the other technologies.

Unlike the other technologies, however, radiative cooling also has the potential to be a completely untethered cooling solution. If a column of liquid is frozen in the container described in Figure 3-8 at a centralized, eco-friendly refrigeration facility, this column can be wheeled into any location without requiring outside access to a condenser, or even a local solar panel array. Of all the solutions posed in this paper, solid-state radiative cooling is the idea that is closest to magic, a trait that has enabled vapor-compression air conditioning to become one of the most important technologies in the world.

Teitelbaum et al. 2020 have implemented this radiative cooling idea for bus stop cooling with promising results as it relates to comfort, drawing roughly 450W to run chilled water through ten 1.2m by 2.1m panels, but no mockup or study has developed a use case focused on the life-saving implementation discussed here.

This radiative cooling concept has two main limitations. First, the performance of the system is extremely sensitive to how well shielded it can be from the surrounding room and how well radiation can be sent towards the human. A physical mockup or simulation is required to validate the view factor numbers estimated in this paper. While they seem reasonable, they only serve as a starting point for discussion in this work. Practical view factors may fully break this design.

The second main limitation is that the outer cylinder material needs to have high transmissivity of wavelengths longer than 2 μm, but also the structural strength to support a vacuum inside. Teitelbaum et al. 2020 found a reduction in transmissivity from 0.84 to 0.25 when increasing their outer surface thickness of their LDPE from 0.05mm to 5mm. It is possible that the strength needed to hold the vacuum could be decoupled with transmissivity, using one strong material to support the hoop stresses, but with built in IR transparent windows sized to survive the vacuum.

As a follow up to this work, the radiative cooling concept can be built using a steady state cold cylinder, that is, a large cylinder of ice. This ice would melt due to the exposure to convective losses, but it will last long enough to allow for measurements of the radiative losses from a human and prove the ability to reflect human radiation into a cold sink. If these results are promising, it could provide justification for investment in solving the outer cylinder material challenge.

One final limitation of this work is minimal exploration of the energy requirements for dehumidification. It is assumed to be large relative to the desired energy values for solar power, based on the magnitude of the water's latent heat of vaporization (2260 kJ/kg).

Lastly, all these solutions are complicated by the nuances of how the human body cools itself. In this paper, the human is treated as a homogeneous block of material with isotropic thermophysical properties. Even ASTM 2003 and ISO 2001 for personal cooling vests use a heated manikin, which is inherently different than how a human would thermally interact with such a device. There is an opportunity to better understand the physiology of cooling to properly leverage how specifically the body should be cooled. Perhaps there are optimal locations to cool a human that minimize energy requirements, such as small phase change packs at specific locations on the skin.

Chapter 5 - Conclusion

This study evaluated if adjustments to status-quo vapor compression air conditioning systems could justify their continued use in an energy constrained, warming world. The findings indicate that these systems will always consume significant amounts of energy due to the physics of cooling air and in turn using that air to keep a human cool. In contrast, low–mass flow rate vapor compression systems, liquid cooling systems, and radiative cooling technologies show potential to cool the human body without requiring an order-of-magnitude increase in energy use. While all three approaches need further development, liquid cooling is closest to practical implementation, whereas radiative cooling is still in its early stages and demands more practical testing. Ultimately, one or more of these alternative systems will be essential for ensuring human resilience in the face of climate change.

Table 5-1: Comparison of Discussed Methods for Cooling a Human
Rows highlighted in blue are most promising

Cooling Method	Peak Energy Draw	Full Day Energy Usage (12h)	Solar Panels Needed	Current Cost	Main Drawback
Single-Stream Air Conditioning	3kW+	-	18+	N/A	Air cooling physics
Full-day air conditioning with recirculation	700-1000W	2-5kWh	6+ or fewer with batteries	$1-2k	Cooling demand extremely dependent on building construction Peak energy draw hard to supply with solar alone
Low Mass Flow Air Conditioning	100-500W	1.2-2.4 kWh	1	$1-2k	Requires custom vapor compression system, condensation from ambient air will increase energy draw, may need to enclose human to separate from room
Solid-State Vests	~400W continuous over hours for small freezer	4-5 kWh assuming overnight phase change	3	$100	Not “on demand” Heat transfer from human may be rate limited May not last all day
Circulating Liquid Vests/Chair	~150-200W	1.8-2.4 kWh	3	$1-2k	Requires custom vapor compression system
Evaporative	1kW+		5+ or fewer with batteries	$1-2k	Energy cost for dehumidification, requires enclosure around body
Radiative	100-300W	1.2-3.6 kWh	1	N/A	Transmissivity of materials Shielding/reflection

Bibliography

Canova, Marcello, Massimo Naddeo, Yuxing Liu, Junqiang Zhou, and Yue-Yun Wang. 2015. "A Scalable Modeling Approach for the Simulation and Design Optimization of Automotive Turbochargers." *SAE International Journal of Engines* 8 (4): 1616–28. https://doi.org/10.4271/2015-01-1288.

Coates, Lucinda, Katharine Haynes, James O'Brien, John McAneney, and Felipe Dimer De Oliveira. 2014. "Exploring 167 Years of Vulnerability: An Examination of Extreme Heat Events in Australia 1844–2010." *Environmental Science & Policy* 42 (October):33–44. https://doi.org/10.1016/j.envsci.2014.05.003.

Epstein, YORAM, YAIR Shapiro, and SHAI Brill. 1986. "Comparison between Different Auxiliary Cooling Devices in a Severe Hot/Dry Climate." *Ergonomics* 29 (1): 41–48. https://doi.org/10.1080/00140138608968239.

Fanger, Poul O. 1972. *Thermal Comfort: Analysis and Applications in Environmental Engineering*. New York: McGraw-Hill.

Gao, Chuansi, Kalev Kuklane, and Ingvar Holmér. 2011. "Cooling Vests with Phase Change Materials: The Effects of Melting Temperature on Heat Strain Alleviation in an Extremely Hot Environment." *European Journal of Applied Physiology* 111 (6): 1207–16. https://doi.org/10.1007/s00421-010-1748-4.

Gaudio, Flavio G., and Colin K. Grissom. 2016. "Cooling Methods in Heat Stroke." *The Journal of Emergency Medicine* 50 (4): 607–16. https://doi.org/10.1016/j.jemermed.2015.09.014.

Giampaolo, Tony. 2023. *Compressor Handbook: Principles and Practice*. 2nd ed. Milton: River Publishers.

Gowen, Annie, Niko Kommenda, Anant Gupta, and Simon Ducroquet. 2023. "Dangerous Heat Waves Expose India's Inequality, Deadly Risk for Poor - Washington Post." The Washington Post. 2023. https://www.washingtonpost.com/climate-environment/interactive/2023/india-deadly-extreme-heat-poverty/.

IEA. 2018. "The Future of Cooling", Paris, https://www.iea.org/reports/the-future-of-cooling, Licence: CC BY 4.0

Jette, F.-X., J.-P. Dionne, J. Rose, and A. Makris. 2004. "Effect of Thermal Manikin Surface Temperature on the Performance of Personal Cooling Systems." *European Journal of Applied Physiology* 92 (6): 669–72. https://doi.org/10.1007/s00421-004-1112-7.

Mansour, Elias, Rotem Vishinkin, Stéphane Rihet, Walaa Saliba, Falk Fish, Patrice Sarfati, and Hossam Haick. 2020. "Measurement of Temperature and Relative Humidity in Exhaled Breath." *Sensors and Actuators B: Chemical* 304 (February):127371. https://doi.org/10.1016/j.snb.2019.127371.

McKenna, Zachary J., Josh Foster, Whitley C. Atkins, Luke N. Belval, Joseph C. Watso, Caitlin P. Jarrard, Bonnie D. Orth, and Craig G. Crandall. 2023. "Age Alters the Thermoregulatory Responses to Extreme Heat Exposure with Accompanying Activities of Daily Living." *Journal of Applied Physiology* 135 (2): 445–55. https://doi.org/10.1152/japplphysiol.00285.2023.

Morris, Nathan B., Georgia K. Chaseling, Timothy English, Fabian Gruss, Mohammad Fauzan Bin Maideen, Anthony Capon, and Ollie Jay. 2021. "Electric Fan Use for Cooling during Hot Weather: A Biophysical Modelling Study." *The Lancet. Planetary Health* 5 (6): e368–77. https://doi.org/10.1016/S2542-5196(21)00136-4.

Oliveira, A. Virgílio M., Adélio R. Gaspar, Sara C. Francisco, and Divo A. Quintela. 2014. "Analysis of Natural and Forced Convection Heat Losses from a Thermal Manikin: Comparative Assessment of the Static and Dynamic Postures." *Journal of Wind Engineering and Industrial Aerodynamics* 132 (September):66–76. https://doi.org/10.1016/j.jweia.2014.06.019.

Pannemans, Daphne L.E., and Klaas R. Westerterp. 1995. "Enegy Expenditure, Physical Activity and Basal Metabolic Rate of Elderly Subjects." *British Journal of Nutrition* 73 (4): 571–81. https://doi.org/10.1079/BJN19950059.

Perkins-Kirkpatrick, S. E., and S. C. Lewis. 2020. "Increasing Trends in Regional Heatwaves." *Nature Communications* 11 (1): 3357. https://doi.org/10.1038/s41467-020-16970-7.

Semenza, Jan C., Carol H. Rubin, Kenneth H. Falter, Joel D. Selanikio, W. Dana Flanders, Holly L. Howe, and John L. Wilhelm. 1996. "Heat-Related Deaths during the July 1995 Heat Wave in Chicago." *New England Journal of Medicine* 335 (2): 84–90. https://doi.org/10.1056/NEJM199607113350203.

Solemma. 2025. "ClimateStudio." Solemma LLC.

Stone, Brian, Carina J. Gronlund, Evan Mallen, David Hondula, Marie S. O'Neill, Mayuri Rajput, Santiago Grijalva, et al. 2023. "How Blackouts during Heat Waves Amplify Mortality and Morbidity Risk." *Environmental Science & Technology* 57 (22): 8245–55. https://doi.org/10.1021/acs.est.2c09588.

Székely, Miklós, Luís Carletto, and András Garami. 2015. "The Pathophysiology of Heat Exposure." *Temperature* 2 (4): 452–452. https://doi.org/10.1080/23328940.2015.1051207.

Teitelbaum, Eric, Kian Wee Chen, Dorit Aviv, Kipp Bradford, Lea Ruefenacht, Denon Sheppard, Megan Teitelbaum, Forrest Meggers, Jovan Pantelic, and Adam Rysanek. 2020. "Membrane-Assisted Radiant Cooling for Expanding Thermal Comfort Zones Globally without Air Conditioning." *Proceedings of the National Academy of Sciences* 117 (35): 21162–69. https://doi.org/10.1073/pnas.2001678117.

Wang, Lijuan, Hui Yin, Yuhui Di, Yanfeng Liu, and Jiaping Liu. 2016. "Human Local and Total Heat Losses in Different Temperature." *Physiology & Behavior* 157:270–76. https://doi.org/10.1016/j.physbeh.2016.02.018.

Winslow, C. -E. A., L. P. Herrington, and A. P. Gagge. 1937. "PHYSIOLOGICAL REACTIONS OF THE HUMAN BODY TO VARYING ENVIRONMENTAL TEMPERATURES." *American Journal of Physiology-Legacy Content* 120 (1): 1–22. https://doi.org/10.1152/ajplegacy.1937.120.1.1.

Yahya, S. M. 2011. *Turbines Compressors and Fans*. 4th ed. New York, N.Y: McGraw-Hill Education LLC.

Yang, Bo. 2022. "Modeling Compressor Pressure Ratio vs. Mass Flow Rate Including Choke Line and Surge Line Using Scaling Theorem." In , 2022-01–0029. https://doi.org/10.4271/2022-01-0029.